

## Low temperature synthesis of CaZrO<sub>3</sub> nanoceramics from CaCl<sub>2</sub>–NaCl molten eutectic salt

Rahman Fazli<sup>1\*</sup> and F. Golestani-Fard<sup>2</sup>

1. Young Researchers and Elite Club, Zanjan Branch, Islamic Azad University, Zanjan, Iran

2. School of Metallurgy and Materials Engineering, Iran University of Science and Technology, Tehran, Iran

Received: 13 Dec. 2014 ; Accepted: 6 May 2015

\*Corresponding Author Email: rhmfazli@yahoo.com, Tel: +98-937-2139453

### Abstract

CaZrO<sub>3</sub> nanoceramics were successfully synthesized at 700 °C using the molten salt method, and the effects of processing parameters, such as temperature, holding time, and amount of salt on the crystallization of CaZrO<sub>3</sub> were investigated. CaCl<sub>2</sub>, Na<sub>2</sub>CO<sub>3</sub>, and nano-ZrO<sub>2</sub> were used as starting materials. On heating, CaCl<sub>2</sub>–NaCl molten eutectic salt provided a liquid medium for the reaction of CaCO<sub>3</sub> and ZrO<sub>2</sub> to form CaZrO<sub>3</sub>. The results demonstrated that CaZrO<sub>3</sub> started to form at about 600°C and that, after the temperature was increased to 1,000°C, the amounts of CaZrO<sub>3</sub> in the resultant powders increased with a concomitant decrease in CaCO<sub>3</sub> and ZrO<sub>2</sub> contents. After washing with hot distilled water, the samples heated for 3 h at 700°C were single-phase CaZrO<sub>3</sub> with 90–95 nm particle size. Furthermore, the synthesized CaZrO<sub>3</sub> particles retained the size and morphology of the ZrO<sub>2</sub> powders which indicated that a template mechanism dominated the formation of CaZrO<sub>3</sub> by molten-salt method.

**Keywords:** calcium zirconate, molten salt method, nanomaterials, template growth.

### 1. Introduction

Calcium zirconate (CaZrO<sub>3</sub>) due to its valuable properties, such as high melting point (2,340°C), high dielectric permittivity, and low dissipation factor, is a ceramic material that is currently being used in a wide range of applications: multilayer ceramic capacitors, solid electrolyte, crystalline host for phosphorescence materials, moderate temperature thermal barrier catalyst, and so on [1–3]. There are several methods for the

synthesis of this material. CaZrO<sub>3</sub> powders is conventionally synthesized via a high temperature (1500°C) solid state reaction of powdered calcium oxide (CaO) (or calcium carbonate (CaCO<sub>3</sub>)) and zirconia (ZrO<sub>2</sub>) (conventional mixed oxide synthesis (CMOS)). As the reactions are generally controlled by slow diffusion mechanisms, highly reactive raw materials, high temperatures, and long duration have to be used for the reactions to

achieve completion. The resultant product is a hard mass, which often needs to be crushed and ground to achieve the desired particle size [4]. Other methods such as electrofusion [5], wet chemical [6–8], combustion [9], and mechanical alloying (MA) [10] have been reported for synthesis of calcium zirconate. Almost all the aforementioned methods are not commodious, because their synthesis temperatures are high in solid state and electrofusion methods and thus need so much thermal energy and time. Therefore, it is necessary to follow methods that decrease synthesis temperature and time. Besides the above techniques, a low temperature synthesis technique called molten salt synthesis (MSS), is beginning to attract interest. In this method, a salt is used as a liquid medium, therefore, the reactions are faster and synthesis is complete in significantly lower temperature and time [4, 11, 12]. Zushu Li *et al.*'s investigation is perhaps the most important research on the synthesis of  $\text{CaZrO}_3$  via molten salt method that prepared  $\text{CaZrO}_3$  powder at  $1,050^\circ\text{C}$  for 5h [4]. In this work,  $\text{CaZrO}_3$  was synthesized by heating  $\text{CaCO}_3$ , sodium carbonate ( $\text{Na}_2\text{CO}_3$ ), sodium chloride ( $\text{NaCl}$ ), and nano- $\text{ZrO}_2$  mixture, and the effects of temperature, holding time, and salt to oxide ratio on synthesis process were investigated. Also, synthesis mechanism was analyzed.

## 2. Experimental Procedure

### 2.1. Dispersion of nano- $\text{ZrO}_2$

Nano- $\text{ZrO}_2$  (Neutrino, Germany,  $D_{50} = 60$  nm, > 99% pure), hydrochloric acid (HCl), and distilled water (pH = 7.2) were used for the dispersion of nano- $\text{ZrO}_2$ . First, pH of distilled water was decreased to 4 using HCl by gently adding it to distilled water and then measuring the pH using pH meter (Jenway, model 3540). After regulating the pH of distilled water, agglomerated nano- $\text{ZrO}_2$  particles were added and stirred for 1h using electrical stirrer. Then, this suspension was placed for 2min in an ultrasonic probe and then stirred for 1h again. The process of stirring and placing in ultrasonic probe were alternatively repeated several times to obtain extremely dispersed particles. Then, a little amount of the stirring suspension was poured on a hot glass lamella using a syringe.

Thereafter, water from the suspension was rapidly vaporized, separated and dispersed particles of nano- $\text{ZrO}_2$  remained in the container. The particle size of dispersed nano- $\text{ZrO}_2$  was determined via dynamic light scattering (DLS, Malvern, ZEN 3600), scanning electron microscopy (SEM, Tescan Vega II), and transition electron microscopy (TEM, CM 200, Philips).

### 2.2. Preparation of powder mixture

$\text{Na}_2\text{CO}_3$  (Merck, Germany,  $D_{50} = 1\text{mm}$ , 99.5% pure), calcium chloride ( $\text{CaCl}_2$ ) (Merck, Germany,  $D_{50} = 4$  mm, 99.5% pure), and nano- $\text{ZrO}_2$  (Neutrino, Germany,  $D_{50} = 60$  nm, > 99% pure) were used as starting materials. First, stoichiometric compositions of  $\text{Na}_2\text{CO}_3$  and  $\text{CaCl}_2$  were completely mixed and the obtained dual mixture was heated at  $150^\circ\text{C}$  for 12h to dry. Then, this salt was added to completely dispersed nano- $\text{ZrO}_2$  solution and the final suspension was stirred for 1 h to homogenize extremely. The mixture was fully dried at  $120^\circ\text{C}$  for 12h. Molar ratio of final mixture was  $\text{ZrO}_2:\text{Na}_2\text{CO}_3:\text{CaCl}_2 = 1:1:1.4$ . Agglomerations of obtained powder which was completely homogenous were broken using an agate mortar and then sifted to pass through a 325 mesh screen ( $45\ \mu\text{m}$ ). Finally, the mixture (20 g) was placed in an alumina crucible covered with an alumina lid, heated to 600; 650; 700; 800; 900; and  $1,000^\circ\text{C}$  and held for 1, 3, and 5h. For investigating the effect of salt to oxide ratio on the synthesis process, the samples were heated at optimum temperature with 1:1, 2:1, 3:1, and 4:1 salt to oxide ratios. The heating and cooling rates were  $3^\circ\text{C}/\text{min}$  and  $5^\circ\text{C}/\text{min}$ , respectively. After cooling to room temperature, the solidified mass was washed and filtered in hot distilled water five times to remove the salts. Then, the obtained powder was dried at  $120^\circ\text{C}$  for 4 h. The phase formation, morphology, and elemental analysis of the synthesized powders were characterized via X-ray diffraction (XRD, Philips pw3710), SEM (TescanVega II), and X-ray fluorescence (XRF, Philips 2404), respectively.

## 3. Results and discussion

### 3.1. Dispersed nano- $\text{ZrO}_2$

SEM micrograph of agglomerated nano- $\text{ZrO}_2$  particles has been shown in Figure 1. It is

obviously observed that particle size of zirconia was in the range of 200–250 nm. This issue can be attributed to adherence and thereupon agglomeration of nano-ZrO<sub>2</sub> particles.

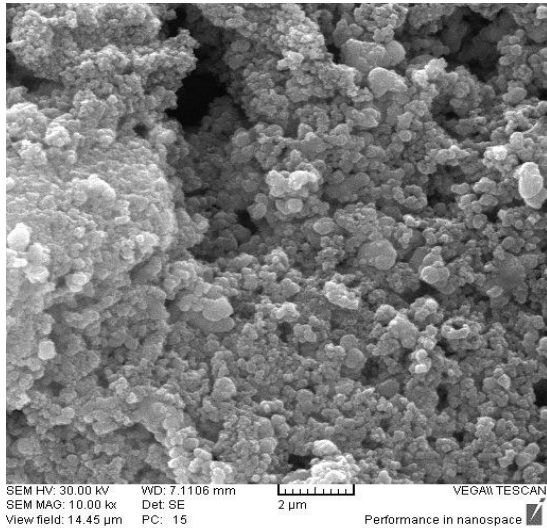


**Fig. 1. SEM micrograph of agglomerated nano-ZrO<sub>2</sub> particles**

SEM micrograph of dispersed nano-ZrO<sub>2</sub> particles has been shown in Figure 2. As seen, particle size of nano-ZrO<sub>2</sub> was in the range of 60–80 nm. This object was confirmed by TEM micrograph of these particles shown in Figure 3.

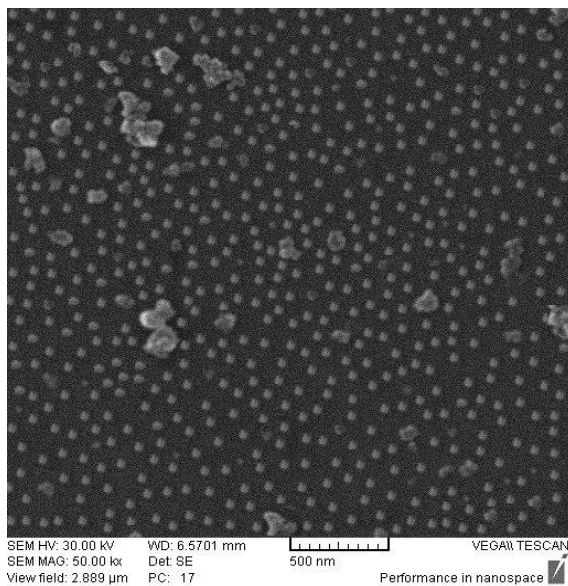


**Fig. 2. SEM micrograph of dispersed nano-ZrO<sub>2</sub> particles**

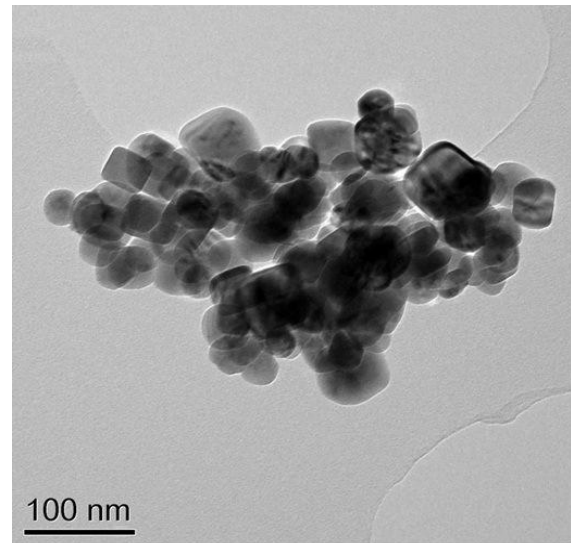


**Fig. 3. TEM micrograph of dispersed nano-ZrO<sub>2</sub> particles**

Figure 4 shows particle size distribution curve of nano-ZrO<sub>2</sub> suspension measured via DLS method. It is seen that distribution of particle size was centralized in the range of 60–70 nm which means that almost all agglomerations were broken and nano-ZrO<sub>2</sub> particles were successfully dispersed.

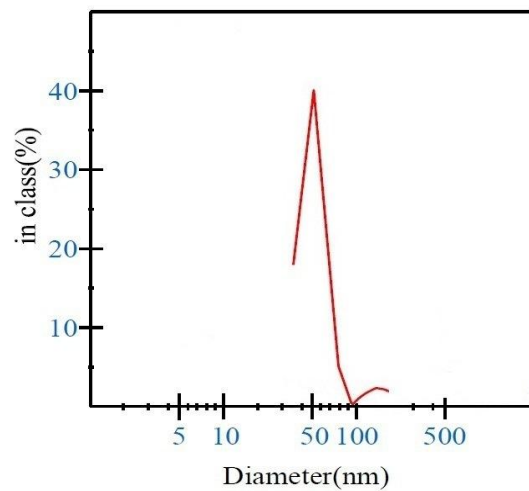


**Fig. 4. Particle size distributing curve of nano-ZrO<sub>2</sub> suspension**

### 3.2. Thermogravimetric analysis (TGA) of synthesis process

DTA/TG analysis was performed to determine the proper reaction temperature range as well as the reaction order in the molten salt method. Figure 5 indicates DTA/TG curve of Na<sub>2</sub>CO<sub>3</sub>,

CaCl<sub>2</sub>, and nano-ZrO<sub>2</sub>. The DTA curve exhibits an endothermic peak (peak a), which is associated with a slow weight loss (10%) in the TG curve at 100°C. This weight loss is attributed to dehydration of the precursors. The small endothermic peak at approximately 150°C (peak b) is related to the reaction between Na<sub>2</sub>CO<sub>3</sub> and CaCl<sub>2</sub>. The big endothermic peak at about 500°C (peak c) is attributed to melting of CaCl<sub>2</sub>-NaCl eutectic salt. The exothermic peak at approximately 600°C (peak d) which is associated with a slow weight loss in the TG curve is related to formation of CaZrO<sub>3</sub>. The small exothermic peak at 700°C (peak e) is interpreted as the crystallization of the CaZrO<sub>3</sub> phase.

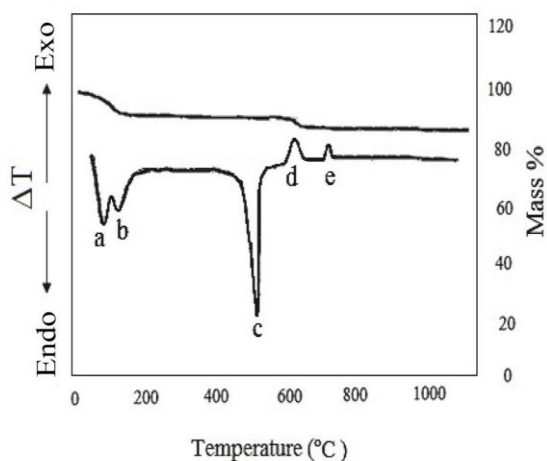


Fig. 5. DTA/TG curve of CaCl<sub>2</sub>, Na<sub>2</sub>CO<sub>3</sub>, and nano-ZrO<sub>2</sub> mixture

### 3.3. Effect of temperature

Figure 6 shows XRD patterns of the samples heated for 3h at different temperatures. As obviously observed, optimum temperature for these samples was 700°C. At this temperature, the samples were single-phase

CaZrO<sub>3</sub> and CaCO<sub>3</sub> and ZrO<sub>2</sub> peaks were not observed. In other words, ZrO<sub>2</sub> and CaCO<sub>3</sub> were completely transformed to CaZrO<sub>3</sub>. At temperatures above 700°C, the samples were likewise single-phase CaZrO<sub>3</sub> and just their crystallinity was increased. This object was confirmed by means of increase in peak's intensity. At 1,000°C, the peak's intensity were insignificantly decreased and partly become wider that can be attributed to acceding decomposition temperature of CaZrO<sub>3</sub>. Thus, increase in temperature was a very effective factor for completion of synthesis process.

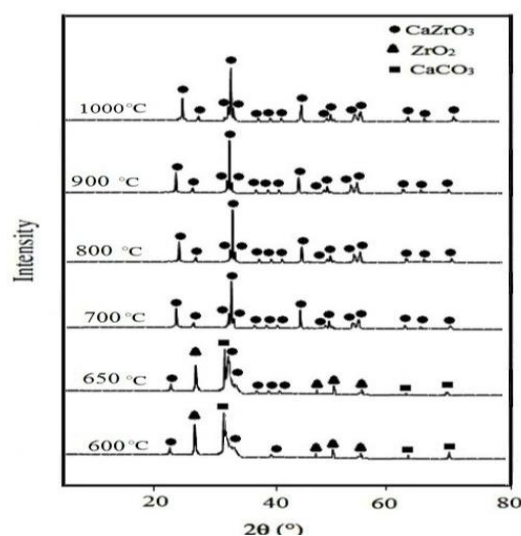


Fig. 6. XRD patterns of the samples (water washed) heated for 3 h at different temperatures

Energy dispersive X-ray spectroscopy (EDS) micrograph of the samples heated at 700°C for 3h shown in Figure 7 confirmed that optimum temperature for synthesized samples was 700°C. As seen, almost only [Ca], [Zr], and [O] elements were observed and other elements were eliminated.

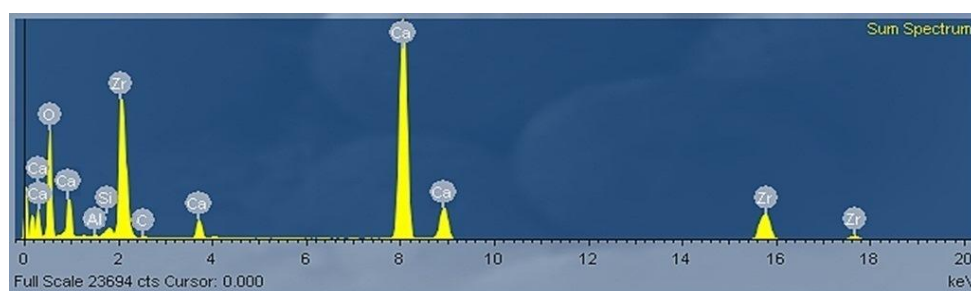


Fig. 7. EDS micrograph of the samples heated at 700°C for 3h

### 3.4. Effect of holding time

Figure 8 provides XRD patterns of the samples heated for different holding times at 700°C. As observed, optimum holding time for these samples was 3 h. In this holding time, synthesis process was complete and the samples were single-phase  $\text{CaZrO}_3$ . Also,  $\text{CaCO}_3$  and  $\text{ZrO}_2$  peaks were not observed. In 1h holding time,  $\text{CaCO}_3$  and  $\text{ZrO}_2$  peaks were seen, in addition to  $\text{CaZrO}_3$  peaks. In other words, synthesis process was not completed. In 5 h holding time, the samples were likewise single-phase  $\text{CaZrO}_3$  and just intensity of their peaks was insignificantly increased compared with 3h holding time, which means that their crystallinity was venially increased. Thus, increase in holding time, before optimum holding time, was an effective factor for completion of synthesis process and after this holding time did not have a significant effect.

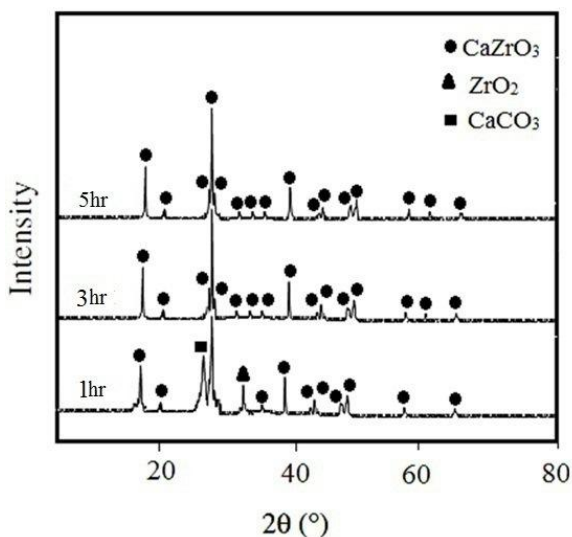


Fig. 8. XRD patterns of the samples (water washed) heated at 700°C with different holding times

### 3.5. Effect of salt amount

XRD patterns of the samples heated with different salt to oxide ratios at 700°C have been shown in Figure 9. It resulted in an optimum salt to oxide ratio of 2:1, as the synthesis process was completed in this ratio. In salt to oxide ratio of 1:1, the samples still did not become single-phase  $\text{CaZrO}_3$ , and it was necessary to increase the salt to oxide ratio for completion of the synthesis. With increase in the salt to oxide

ratio of 2:1 to higher values, the samples remained single-phase and during more increase in salt to oxide ratio, more increase in peaks intensity and thereupon more increase in crystallinity property were seen. Thus, increase in salt to oxide ratio was a very effective factor for the completion of synthesis process.

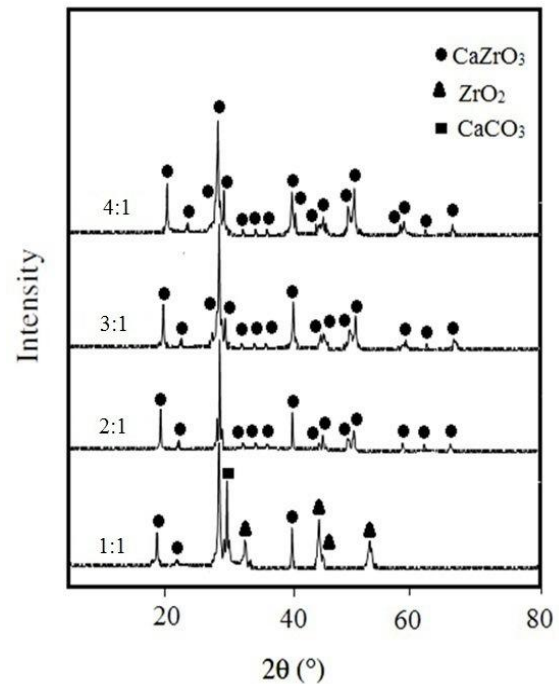


Fig. 9. XRD patterns of the samples (water washed) heated at 700 °C for 3 h with different salt to oxide ratios

### 3.6. Particle size

Figure 10 shows SEM micrographs of the samples synthesized at different temperatures. As seen, the particle size of  $\text{CaZrO}_3$  synthesized at 700, 800, and 900°C was in the range of 90–95 nm. Whereas, the particle size of  $\text{CaZrO}_3$  synthesized at 1,000°C was in the range of 180–200 nm which can be attributed to grain growth phenomenon started at above 1,000°C.

Particle size distribution curve of  $\text{CaZrO}_3$  particles synthesized at 700°C for 3h measured via DLS method has been shown in Figure 11. As seen, distribution of particle size was centralized in the range of 90–95 nm.

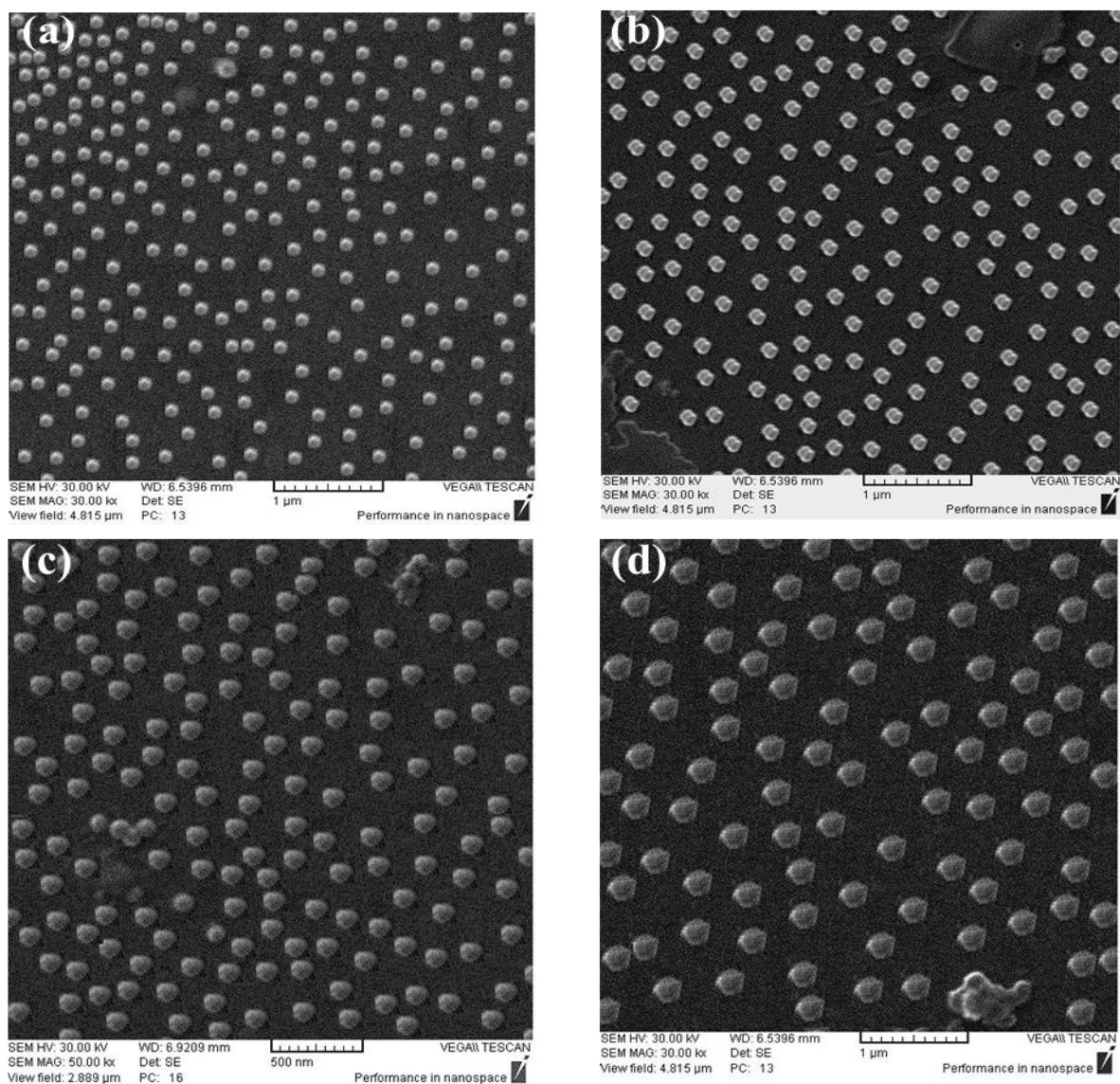


Fig. 10. SEM micrographs of the samples synthesized for 3 h at (a) 700°C; (b) 800°C; (c) 900°C; (d) 1,000°C

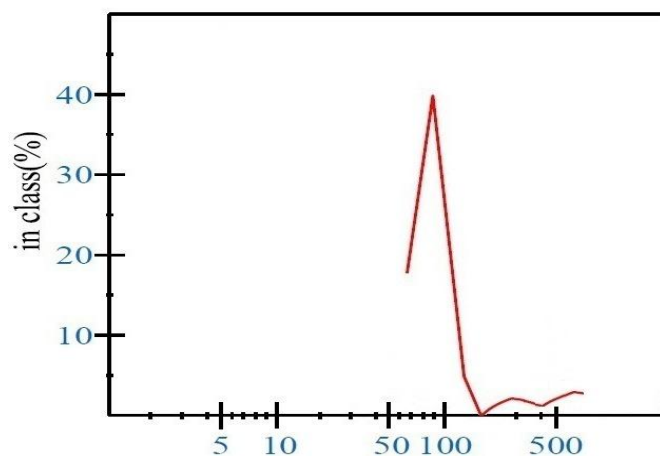


Fig. 11. Particle size distribution curve of CaZrO<sub>3</sub> particles synthesized at 700°C for 3h

### 3.7. CaZrO<sub>3</sub> synthesis mechanism

NaCl, CaCl<sub>2</sub>, or NaCl–CaCl<sub>2</sub> salts could be used as molten salt media. According to Figure 12 [13], as melting point of eutectic salt

(504°C) was lower than both singular CaCl<sub>2</sub> (771°C) and NaCl (801°C) salts, NaCl–Na<sub>2</sub>CO<sub>3</sub> eutectic salt was more suitable.

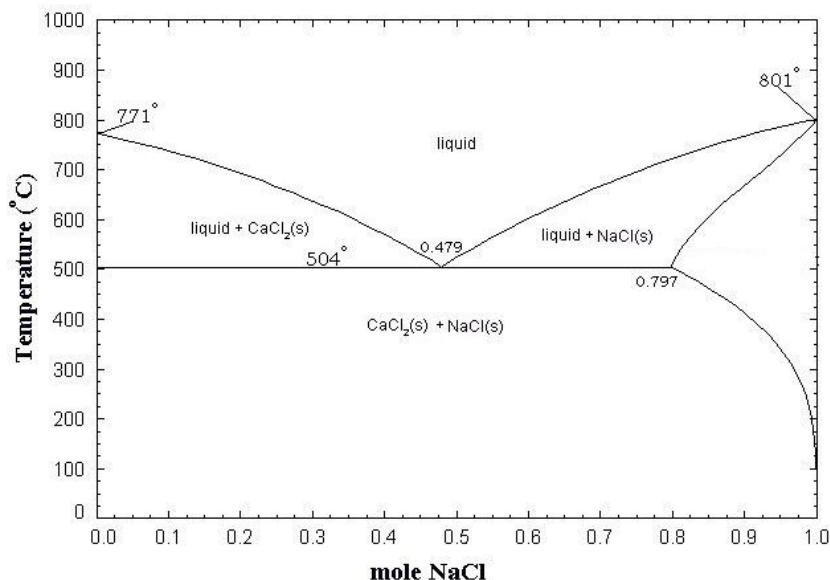
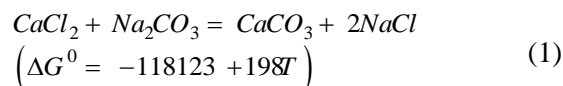


Fig. 12. CaCl<sub>2</sub>–NaCl phase diagram [14]

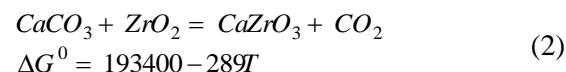
On heating the mixture, the first reaction was between Na<sub>2</sub>CO<sub>3</sub> and CaCl<sub>2</sub> (Reaction 1).



This is consistent with the thermodynamic prediction that reaction 1 could occur at as low as room temperature, because the  $\Delta G^0$  is negative in the whole temperature range between 25 and 600°C [14]. Once Reaction (1) was completed, Na<sub>2</sub>CO<sub>3</sub> would disappear, and the salt assembly would become one that is essentially composed of NaCl and excess CaCl<sub>2</sub>. The molar ratio between NaCl and the excess of CaCl<sub>2</sub> is 2:0.4, and the NaCl–CaCl<sub>2</sub> phase diagram indicates that salt with such a composition will start to melt at 504°C (eutectic temperature) in the areas where the eutectic exists and become completely liquid at about 650°C (liquidus temperature).

This molten NaCl–CaCl<sub>2</sub> salt provided a reaction medium for the CaZrO<sub>3</sub> synthesis and also acted as a very proper catalyzer. Thus, Reaction 2 started at about 600°C that was very lower than its thermodynamic prediction (670°C) [14]. With increase in the

temperature to 600°C, CaCO<sub>3</sub> reacted with ZrO<sub>2</sub> and some CaZrO<sub>3</sub> was formed. With increase in the temperature to 650°C, NaCl–CaCl<sub>2</sub> salt completely melted, and reaction 2 became very more complete and rapid. Due to very high reactivity of nano size ZrO<sub>2</sub>, synthesis of CaZrO<sub>3</sub> was completed at 700°C.



To understand the reaction mechanisms, the whole synthesis process of CaZrO<sub>3</sub> discussed above has schematically been illustrated in Figure 13.

Two main mechanisms, “template-growth” and “dissolution-precipitation,” were involved in MSS. Solubility of reactants in the molten salt plays an important role in MSS. This not only affects the reaction rate but also the morphologies of the synthesized particles. If both of the reactants are soluble in the molten salt, then the product phase will be readily synthesized via precipitation from the salt containing the dissolved reactants (dissolution–precipitation mechanism). In this case the morphologies of the product grains will generally be different from those of the

reactants. However, if one of the reactants is much more soluble than another, the more soluble reactant will dissolve into the salt firstly and then diffuse onto the surfaces of the less

soluble reactant and react in situ to form the product phase. In this case, the morphology of the synthesized grain will retain the less soluble reactant (template-growth mechanism) [15, 16].

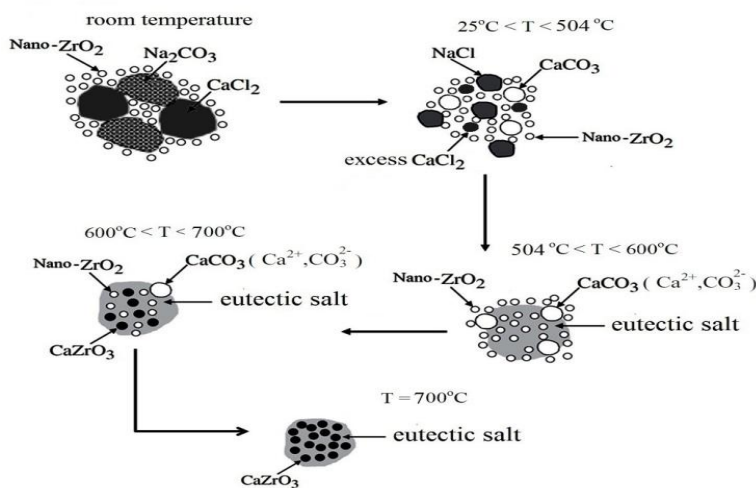


Fig. 13. Schematic diagram illustrating the synthesis of CaZrO<sub>3</sub> powder by heating nano ZrO<sub>2</sub>, CaCl<sub>2</sub>, and Na<sub>2</sub>CO<sub>3</sub>

According to some studies [17, 18], CaCO<sub>3</sub> is soluble in a chloride molten salt. Its solubility in a NaCl-based salt at 700–1,000°C are on the order of 10<sup>-3</sup> (molar fraction), which is thousand times higher than that of ZrO<sub>2</sub> (on the order of 10<sup>-6</sup>). Therefore, during the MSS process, CaCO<sub>3</sub> would be dissolved more in the NaCl–CaCl<sub>2</sub> molten salt and react with ZrO<sub>2</sub> templates to form *in situ* CaZrO<sub>3</sub>. This explains the similarity between the grain shapes of the synthesized CaZrO<sub>3</sub> and original ZrO<sub>2</sub> powder. The morphology and particle size of the synthesized CaZrO<sub>3</sub> grains was similar to

ZrO<sub>2</sub> grains which mean that the “template-growth” mechanism played a dominant role in the low-temperature molten salt synthesis of CaZrO<sub>3</sub> nanoparticles (Fig. 14).

The chemical composition of product powders determined via XRF analysis has been shown in Table 1. As seen, after washing, only minor contents of salt and other contaminations remained in the synthesized CaZrO<sub>3</sub> powders. The main objective of this table is to illustrate the feasibility of the molten salt method for the synthesis of very pure ceramic powders.

Table 1. Chemical composition of synthesized CaZrO<sub>3</sub> in different reaction conditions

Weight Percent							Reaction Condition		
Al	C	Cl	Si	O	Zr	Ca	Salt to oxide ratio	Time (h)	Temperature (°C)
0.01	0.03	0.08	0.14	59.92	19.89	19.93	2:1	3	600
0.01	0.02	0.08	0.12	59.93	19.90	19.94	2:1	3	650
0.02	0.01	0.07	0.13	59.93	19.91	19.93	2:1	3	700
0.01	0.01	0.08	0.11	59.92	19.92	19.95	2:1	3	800
0.02	0.02	0.07	0.12	59.91	19.92	19.94	2:1	3	900
0.02	0.03	0.06	0.12	59.91	19.91	19.95	2:1	3	1000
0.01	0.03	0.08	0.11	59.92	19.91	19.94	2:1	1	700
0.01	0.02	0.07	0.11	59.90	19.93	19.96	2:1	5	700
0.01	0.01	0.08	0.12	59.91	19.92	19.95	1:1	3	700
0.01	0.01	0.07	0.12	59.92	19.91	19.96	3:1	3	700
0.01	0.01	0.07	0.13	59.92	19.90	19.96	4:1	3	700



#### 4. Conclusions

1. Nano-size calcium zirconate powders were synthesized via molten salt method.  $\text{Na}_2\text{CO}_3$ ,  $\text{CaCl}_2$ , and nano-  $\text{ZrO}_2$  were used as starting materials.

2. Optimum temperature for samples was  $700^\circ\text{C}$  that was significantly lower than that required by solid state method. Increase in temperature was a very effective factor for completion of synthesis process.

3. Optimum holding time for samples was 3h. Increase in holding time significantly did not affect synthesis process.

4. Optimum salt to oxide ratio for samples was 2:1. Increase in salt to oxide ratio resulted in increase in the crystallinity property. Also, increase in salt to oxide ratio was an effective factor for completion of synthesis process.

5. Particle size of synthesized  $\text{CaZrO}_3$  was 90–95 nm. At above  $1,000^\circ\text{C}$ , grain growth phenomenon caused increase of particle size.

6. Similarity of morphology and particle size of synthesized  $\text{CaZrO}_3$  to  $\text{ZrO}_2$  grains showed that “template–growth” was dominant mechanism in synthesis process.

7. Very minor contaminations components remained in the synthesized powders indicated that very pure  $\text{CaZrO}_3$  nanoceramics was formed from  $\text{CaCl}_2$ – $\text{NaCl}$  molten eutectic salt.

#### References

- [1]. G. Ro'g, M. Dudek, A. Kozłowska-Ro'g, M. Buc'ko, Calcium zirconate: preparation, properties and application to the solid oxide galvanic cells, *J. Electrochimica Acta.* 47 (2002) 4523- 4529.
- [2]. T. Yu, C. H. Chen, X. F. Chen, W. Zhu, R. G. Krishnan, Fabrication and characterization of perovskite  $\text{CaZrO}_3$  oxide thin films, *Ceram. Int.* 30 (2004) 1279-1282.
- [3]. W.J. Lee, A. Wakahara, B.H. Kim, Decreasing of  $\text{CaZrO}_3$  sintering temperature with glass frit addition, *Ceram. Int.* 31 (2005) 521-524.
- [4]. Z.S. Li, W.E. Lee, S. Zhang, Low temperature synthesis of  $\text{CaZrO}_3$  powder from molten Salts, *J. Am. Ceram. Soc.* 90 (2007) 364-368.
- [5]. Z. Song, Q. Li, D. Ma, J. Wen, F. Yuan, and S. Deng, Production Process for Electrically Fused Calcium Zirconate China patent. page 6 (2003).
- [6]. C. Moure, L.D. Olmo, G.F. Arroyo, P. Duran, J. R. Jurado, C. Pascual, Sintering and Densification of Calcium Zirconate Powders Prepared by Coprecipitation, *Science of Ceram.* 12 (1984) 321-326.
- [7]. G. Pfaff, Wet Chemical Synthesis of the Calcium Zirconates  $\text{CaZrO}_3$  and  $\text{CaZr}_4\text{O}_9$ , *Mater.Sci.* 3 (2002) 59-67.
- [8]. F. Gonenli , A. C. Tas, Chemical Synthesis of Pure and Gd-Doped  $\text{CaZrO}_3$  Powders, *J. Eur. Ceram. Soc.* 19 (1999) 2563-2567.
- [9]. R. Ianos, P. Barvinschi, Solution combustions synthesis of calcium zirconate,  $\text{CaZrO}_3$ , powders, *J. Solid State Chem.* 183 (2010) 491-496.
- [10]. S. K. Manik, S. K. Pradhan, X-ray Microstructure Characterization of Ball-Milled Nanocrystalline Microwave Dielectric  $\text{CaZrO}_3$  by Rietveld Method *J. Appl. Crystallogr.* 38 (2004) 291-298.
- [11]. Z. Song, J. Ma, H. Sun, W. Wang, Y. Sun, L. Sun, Z. Liu, C. Gao, Synthesis of  $\text{NiWO}_4$  nanoparticles in low temperature molten salt medium, *Ceram. Int.* 35 (2009) 2675-2678.
- [12]. X. Jiang, J. Ma, Y. Yao, Y. Sun, Z. Liu, Y. Ren, J. Liu, B. Lin, Low temperature synthesis of  $\text{SrWO}_4$  nano-particles by a molten salt method, *Ceram. Int.* 35(2009) 3525-3528.
- [13]. R. S. Roth, M. A. Clevinger, and D. McKenna, Phase Diagrams for Ceramists, Edited by Smith G. American Ceramic Society, (1984) 63-66.
- [14]. J. Kubaschewski, C.B. Alcock, Metallurgical Thermochemistry, 5th edition, Pergamon Press, Oxford, (1979).
- [15]. Z. Li, S. Zhang, W.E. Lee, Molten salt synthesis of  $\text{LaAlO}_3$  powder at low temperatures, *J. Eur. Ceram. Soc.* 27 (2007) 3201-3205.
- [16]. Z. Li, S. Zhang, W.E. Lee, Molten salt synthesis of zinc aluminate powder, *J. Eur. Ceram. Soc.* 27 (2007) 3407-3412.
- [17]. T.P. Boyarchuk, E.G. Khailova, V.L. Cherginets, Potentiometric Measurements in Molten Chlorides Solubilities of Metal Oxides in the Molten Eutectic Mixture  $\text{CsCl}$ – $\text{KCl}$ – $\text{NaCl}$  at  $600^\circ\text{C}$ , *J. Electrochim Acta.* 38 (1993) 1481-1485.
- [18]. V.L. Cherginets, E.G. Khailova, On the Solubility of Bivalent Metal Oxides in Molten Alkaline Chlorides, *J. Electrochim Acta.* 39 (1994) 823-829.